Bidirectional DC-DC Converter Design and Implementation for Lithium-ion Battery Application

Ya-Xiong Wang, Fei-Fei Qin, and Young-Bae Kim
Dept. of Mechanical Engineering
Chonnam National University
Gwangju 500-757, Republic of Korea
yaxiongwang@hotmail.com, hellofeifei@naver.com, ybkim@chonnam.ac.kr

Abstract— **Bidirectional DC-DC converter is potentially used for an energy charging or discharging device; however, the converter displays highly non-linear characteristics since its internal system parameter varies depending on the operation mode and the disturbance engagement. To cope with the non-linearity, a bidirectional DC-DC converter based on time delay control (TDC) is designed and validated for lithium-ion battery application. Control-oriented lithium-ion battery-fed bidirectional DC-DC converter model is constructed with MATLAB/Simulink. Converter PWM duty ratio control technique based on TDC is subsequently designed and assembled for lithium-ion battery operation regulation. Moreover, to validate the efficacy of the present approach, proportional-integral (PI) control is implemented and its results are compared with TDC results. The experimental implementation is performed with *National Instrument* (NI) LabVIEW, whose results show excellent bidirectional converter performance.**

Index Terms--**Bidirectional DC-DC converter, battery discharge, battery recharge, time delay control (TDC), disturbance rejection.**

I. INTRODUCTION

Renewable energy serving as an alternative power solution with zero emission power generation has been increasingly attracted attention in the automotive filed [1]–[3]. Energy storage devices, such battery or super-capacitor, are widely applied to store or supply power to satisfy the energy balance between main power source (i.e., renewable energy like photovoltaic array and fuel cell) and load demand. However, the load requirement varies rapidly in the vehicular application, for example, the fast discharge and recharge is compulsory for an energy storage device. Meanwhile, bidirectional DC-DC converter is proposed to condition voltage and/or current of energy storage device depending on the discharging or charging process to cope with the varied operation points [4], [5]. Moreover, bidirectional converter exhibits challenging control problems, since it possesses highly non-linear characteristics and it involves frequent mode variation. Therefore, this study proposes a new approach for the bidirectional DC-DC converter PWM duty ratio control based on time delay control (TDC) to regulate lithium-ion battery discharging and charging effectively.

Several studies have been carried out for bidirectional DC-DC converter voltage and/or current regulation [6]–[12]. Proportional-integral (PI) control is typically utilized for tracking bidirectional converter reference voltage or current [5]–[7]; however, the converter operation mode including boost type and buck type varies unpredictably determined by energy distribution, which results in highly non-linear characteristics that cause inferior performance governed by linear controller. Consequently, adaptive PI control [8], sliding-mode control (SMC) [9], [10], model predictive control (MPC) [11] and fuzzy logic control (FLC) [12] are developed to address the operation condition change. Novel non-linear control approaches like dynamic evolution control (DEC) [13], [14], filter-combined SMC [15], and gain scheduling control [16], are introduced to improve bidirectional converter control performance recently. TDC is a well-known non-linear control method that was originally developed by Youcef-Toumi [17]. Wang *et al.* [18], [19] used TDC to regulate boost-type and buck-type converters output voltage with superior performance that displays good disturbance rejection results. Therefore, TDC is selected for manipulating bidirectional DC-DC converter PWM duty ratio.

The organization of the paper is as follows. Section II provides lithium-ion battery supplied bidirectional converter system modeling. Section III describes TDC controller and PI controller design method. Numerical simulation and experimental implementation are given in section IV. Section V draws the conclusion of this study.

II. SYSTEM CONTROL-ORIENTED MODEL

The proposed power system is composed of lithium-ion battery, bidirectional converter and external load. System configuration of the lithium-ion battery fed bidirectional DC-DC converter is shown in Fig. 1. The converter is used for stepping-up output voltage when load demand is large, whereas the converter is served as a buck mode to protect battery with optimal charging voltage.

This work was supported by the National Research Foundation of Korea (NRF) funded by the Ministry of Education (2013-0005339), and by the Brain Korea 21 PLUS (BK 21+).

978-1-4799-7537-2/14/$31.00 ©2014

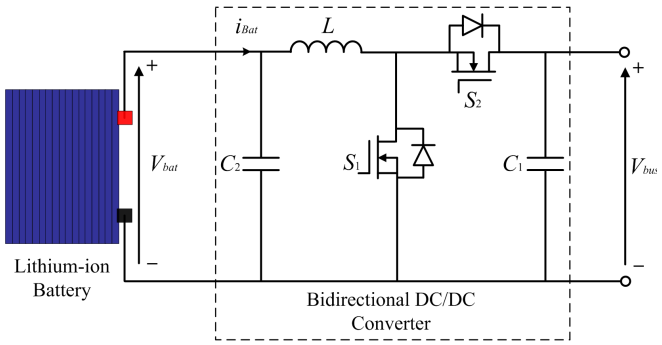

Fig. 1. Lithium-ion battery fed bidirectional DC-DC converter system configuration

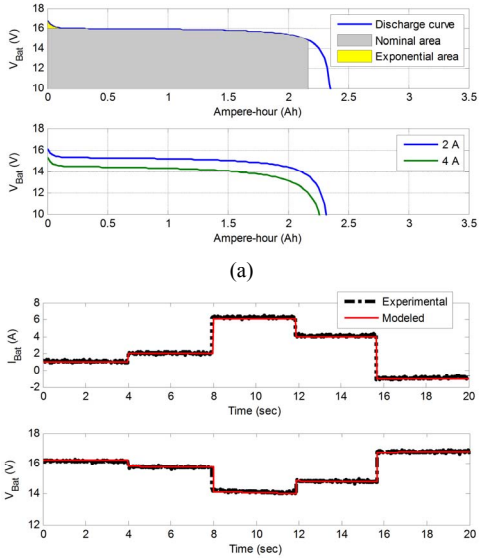

(a)

(b)

Fig. 2. Lithium-ion battery modeling: (a) Battery discharge characteristics (b) Modeling and experimental results comparison

A. Model of Lithium-ion Battery

The model of a lithium-ion battery is comprised of discharge mode and charge mode. The battery block model in MATLAB/Simulink shows good accuracy; therefore, it can be easily selected for representing lithium-ion battery model. The discharge mode of battery voltage is expressed by [7], [20]

$$V_{bat} = E_0 - \frac{K \cdot Q}{Q - it} \cdot i^* - \frac{K \cdot Q}{Q - it} \cdot it + A \cdot \exp\left(-B \cdot it\right) \quad (1)$$

The charge mode is obtained by [7], [20]

$$V_{bat} = E_0 - \frac{K \cdot Q}{it + 0.1Q} \cdot i^* - \frac{K \cdot Q}{Q - it} \cdot it + A \cdot \exp\left(-B \cdot it\right) \quad (2)$$

in above equations, E_0 is the battery constant voltage, K is the polarization constant, Q represents the maximum battery capacity, it denotes the extracted capacity and is described by $it = \int idt$, i^* is the filtered battery current, and A and B represent exponential voltage and capacity, respectively [7], [20].

The nominal voltage and nominal capacity of the applied lithium-ion battery are 14.8 V and 2400 mAh, respectively. Fig. 2(a) indicates the discharge curve characteristics of the lithium-ion battery. Fig. 2(b) shows dynamic response comparison between modeling and experimental results. The dynamic model fitting shows excellent accuracy in compared with the real battery model.

TABLE I
PARAMETERS OF BIDIRECTIONAL CONVERTER

Symbol	Description	Value
L	Bidirectional converter inductance	500 μH
C_1	Bidirectional converter capacitance for boost mode	200 μF
C_2	Bidirectional converter capacitance for buck mode	500 μF
f_{S1}	MOSFET switch S_1 PWM frequency	30 kHz
f_{S2}	MOSFET switch S_2 PWM frequency	30 kHz

B. Modeling of Bidirectional DC-DC Converter

The schematic diagram of bidirectional DC-DC converter is shown in Fig. 1. The converter is assumed working on a continuous operation mode. When MOSFET S_1 is active and MOSFET S_2 is used as a diode element, bidirectional converter serves as a boost mode for stepping up output voltage to supply the load demand. On the other hand, when MOSFET S_2 is active and MOSFET S_1 acts as a diode, the converter indicates voltage stepping down operation resulting in the battery charge mode whose external power is supplied from breaking energy for a vehicular application. The bidirectional converter dynamics model is given by the following equations:

for the boost mode (S_1 is active, and S_2 acts as a diode):

$$\begin{bmatrix} \dot{x}_1 \\ \dot{x}_2 \end{bmatrix} = \begin{bmatrix} 0 & -\frac{1}{L} \\ \frac{1}{C_1} & -\frac{1}{R_{load} C_1} \end{bmatrix} \begin{bmatrix} x_1 \\ x_2 \end{bmatrix} + \begin{bmatrix} \frac{x_2}{L} \\ -\frac{x_1}{C_1} \end{bmatrix} u_1 + \begin{bmatrix} \frac{1}{L} \\ 0 \end{bmatrix} x_3 \quad (3)$$

for the buck mode (S_2 is active, and S_1 acts as a diode):

$$\begin{bmatrix} \dot{x}_1 \\ \dot{x}_3 \end{bmatrix} = \begin{bmatrix} 0 & -\frac{1}{L} \\ \frac{1}{C_2} & -\frac{1}{R_{bat} C_2} \end{bmatrix} \begin{bmatrix} x_1 \\ x_3 \end{bmatrix} + \begin{bmatrix} \frac{x_2}{L} \\ 0 \end{bmatrix} u_2 \quad (4)$$

where $\boldsymbol{x}=\begin{bmatrix} i_L & V_{bus} & V_{bat} \end{bmatrix}^T$ is the state vector, and i_L, V_{bus} and V_{bat} denote the inductor current, the DC link voltage, and the battery voltage, respectively. The parameters of above-mentioned bidirectional converter are listed in Table I.

III. BIDIRECTIOANAL CONVERTER VOLTAGE REGULATION

To regulate lithium-ion battery charging voltage and to provide constant DC bus voltage, TDC is employed to manipulate bidirectional DC-DC converter.

A. Time Delay Control (TDC)

TDC is using time-delayed system information to replace unknown dynamics and disturbance, where the delayed time is assumed as an insignificant value. The detailed introduction and deduction of TDC were discussed in Refs [17]-[19]. The control input $u(t)$ of general TDC form is given by [17]-[19]:

$$u(t) = B^{+}(x(t),t)\{-f(x(t),t) - \dot{x}(t-T) + f(x(t-T),t-T) + B(x(t-T),t-T)u(t-T) + \dot{x}_m(t) - A_e e(t) \quad (5)$$

where $\boldsymbol{f}(\boldsymbol{x}(t),t)$ is the system known dynamics at time instant t, $\boldsymbol{B}$ and $\boldsymbol{B}^{+}$ are the input matrix and pseudo-inverse of input matrix, respectively, T is delayed-time interval, $\boldsymbol{x_m}(t)$ is the state vector of reference model, and $\boldsymbol{A_e}$ and $\boldsymbol{e}(t)$ are the error dynamics and error vector, respectively.

B. TDC for Bidirectional Converter Voltage Regualtion

The control purpose of bidirectional DC-DC converter is regulating both DC link bus voltage and battery charging voltage to satisfy load demand and protect battery from over-charging. Reference model is first selected for the application of TDC, and its reference vector is shown below:

$$x_m = \begin{bmatrix} i_{L,ref} \\ V_{bus,ref} \\ V_{bat,ref} \end{bmatrix} \quad (6)$$

where the reference values of the current and the voltage are constant rendering the derivate of reference model $\dot{x}_m = 0$.

Based on Eq. (5), the PWM control input for a boost mode is calculated by:

$$u_1(t) = \frac{V_{bus}(t) - L\hat{\dot{i}}_L(t-T) + V_{bus}(t-T)[u_1(t-T)-1]}{V_{bus}(t)} - \frac{LK\left[V_{bus,ref} - V_{bus}(t)\right]}{V_{bus}(t)} \quad (7)$$

and PWM duty ratio for a buck mode is given by:

$$u_2(t) = \frac{V_{bat}(t) - L\hat{\dot{i}}_L(t-T) + V_{bus}(t-T)u_2(t-T)}{V_{bus}(t)} - \frac{V_{bat}(t-T) - LK\left[V_{bat,ref} - V_{bat}(t)\right]}{V_{bus}(t)} \quad (8)$$

where $\hat{\dot{i}}_L$ is numerical estimation of inductor current derivate, which is calculated by:

$$\hat{\dot{i}}_L = \frac{i_L(t) - i_L(t-2T)}{2T} \quad (9)$$

C. PI Control for Bidirectional Converter Voltage Regulation

PI control is also applied to regulate bidirectional converter voltages for comparison. The controller is given by the following form:

for boost mode,

$$u_1(t) = K_{P_1}\left[V_{bus,ref} - V_{bus}(t)\right] + K_{I_1}\int\left[V_{bus,ref} - V_{bus}(t)\right]dt \quad (10)$$

for buck mode,

$$u_2(t) = K_{P_2}\left[V_{bat,ref} - V_{bat}(t)\right] + K_{I_2}\int\left[V_{bat,ref} - V_{bat}(t)\right]dt \quad (11)$$

TABLE II
BIDIRECTIONAL CONVERTER TEST CONDITIONS

Conditions	Variation description
Case 1	Mode change (buck mode to boost mode)
Case 2	Reference voltage change (24 V to 28 V) on boost mode
Case 3	Load demand change (0.1 A to 3 A) on boost mode
Case 4	Reference voltage change (18 V to 19.5 V) on buck mode
Case 5	Bus voltage change (20 V to 24V) on buck mode

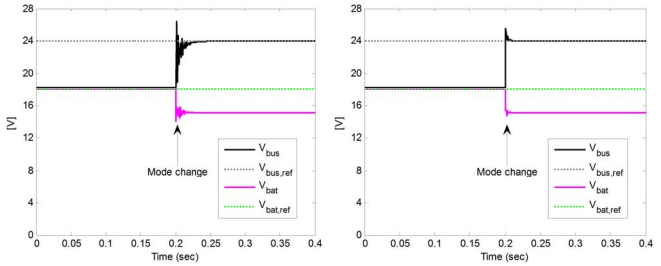

(a) (b)

Fig. 3. Bidirectional converter mode change performance: (a) PI control; (b) TDC.

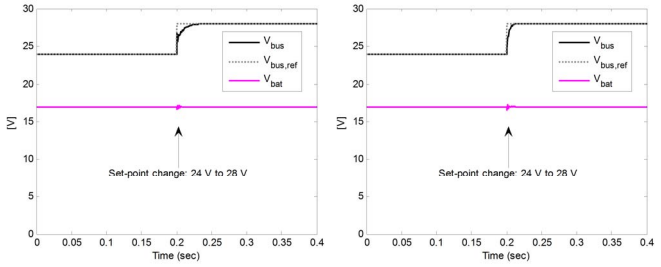

(a) (b)

Fig. 4. Bidirectional converter reference voltage change performance on boost mode operation: (a) PI control; (b) TDC.

IV. NUMERICAL SIMULATION AND EXPERIMENTAL IMPLEMENTATION

Numerical simulations were carried out in MATLAB/Simulink based on the control-oriented model and its controllers. To test the proposed control method, disturbance rejection performances were compared. The test conditions are summarized in Table II. Moreover, experimental implementation was also performed in the same conditions.

A. Numerical Simulation

The mode change control was firstly tested as shown in Fig. 3. The figure shows the mode change response. Before 0.2 sec, bidirectional converter was acting as a buck converter, and battery is charged under the reference voltage (18 V). After 0.2 sec, the load increased suddenly, and the bidirectional converter operates as a boost converter. The output of a lithium-ion battery steps up to bus voltage of the setpoint (24 V). Both PI control and TDC show the achievement of the mode change requirement as shown in Fig. 3(a) and Fig. 3(b), while TDC indicates better performance with smaller voltage ripple and overshoot compared to PI control. Subsequent test conditions are applied to the bidirectional converter on boost mode and buck mode, respectively. Case 2 control performance for both controllers

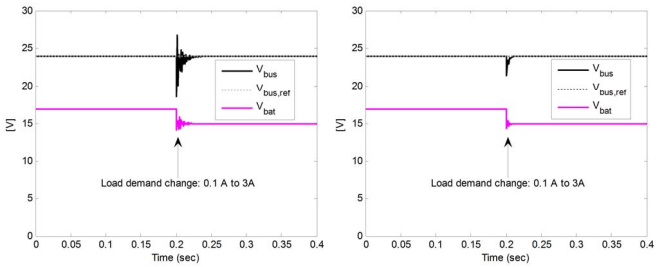

(a) (b)

Fig. 5. Bidirectional converter disturbance rejection performance on boost mode operation: (a) PI control; (b) TDC.

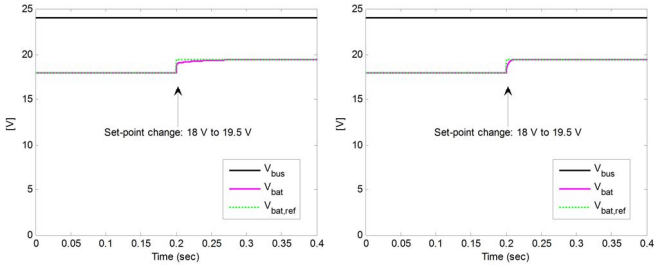

(a) (b)

Fig. 6. Bidirectional converter reference voltage change performance on buck mode operation: (a) PI control; (b) TDC.

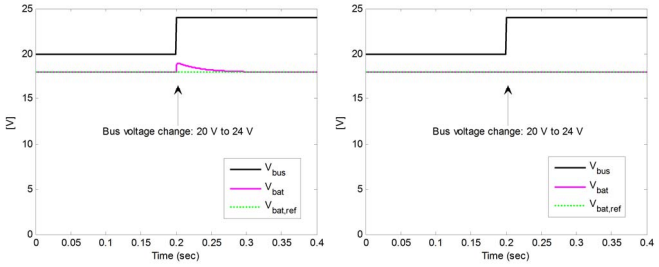

(a) (b)

Fig. 7. Bidirectional converter DC link bus voltage change performance on buck mode operation: (a) PI control; (b) TDC.

are given in Fig. 4. The reference voltage was changed from 24 V to 28 V at 0.2 sec. TDC takes 0.026 sec to settle to the new setpoint, while settling time for PI control is 0.061 sec. TDC shows better performance in test condition of case 2 also. The disturbance rejection results are presented in Fig. 5. PI control shows inferior performance with large voltage ripples and overshoot, while TDC gives a better result with little ripples and overshoot. Buck mode tests are carried out under test conditions of case 4 and 5. When battery charge voltage setpoint varies from 18 V to 19.5 V at 0.2 sec, TDC shows faster settling time. Moreover, TDC-based buck mode output voltage is not determined by bus voltage change (i.e., from 20 V to 24 V) since battery voltage has no variation in Fig. 7 (b), while PI control indicates overshoot to respond the supply voltage changing.

B. Experimental Implementation

Experimental implementation is finally performed with *National Instrument* (NI) LabVIEW-based test rig, lithium-ion battery, DC electronic load, and bidirectional DC-DC converter. The test condition is the same as the simulation one which is listed in Table II. Mode change is tested with its results are shown in Fig. 8. PI control shows relatively large

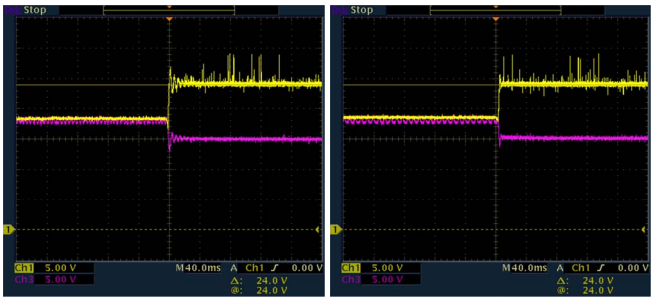

(a) (b)

Fig. 8. Bidirectional converter mode change performance by experiment: (a) PI control; (b) TDC.

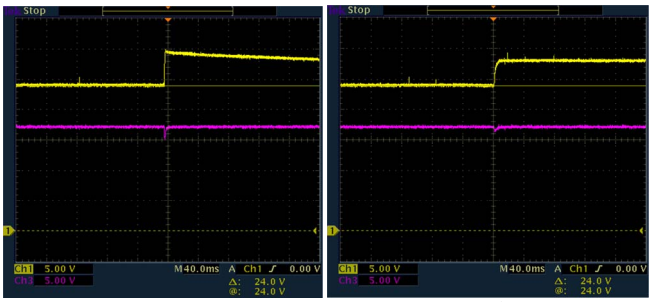

(a) (b)

Fig. 9. Bidirectional converter reference voltage change performance on boost mode operation by experiment: (a) PI control; (b) TDC.

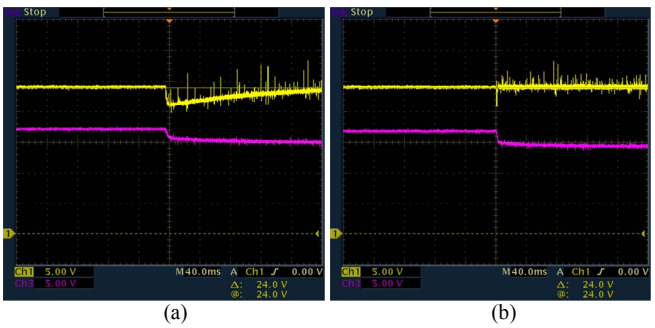

(a) (b)

Fig. 10. Bidirectional converter disturbance rejection performance on boost mode operation by experiment: (a) PI control; (b) TDC.

ripples in comparison with TDC, which is similar to the simulation result. Fig. 9 gives the reference output voltage change, and the result shows a little difference from simulation, where the ripple is significantly reduced but settling time is much longer than simulation result. TDC has much faster disturbance rejection ability for a boost mode, where TDC settling time was 0.24 sec shorter than PI control. Fig. 11 and Fig. 12 show the buck mode test results. The setpoint change performance in PI control and TDC is similar. The settling time is approximately 6 ms for both PI control and TDC. The disturbance rejection test is validated by changing bus voltage from 20 V to 24 V at 0.2 sec. TDC shows 1 V overshoot and 8 ms settling time, whereas PI control overshoot voltage is 0.9 V with 0.22 sec settling time. In conclusion, TDC shows better experimental performance than PI control under test cases of 1~5.

V. CONCLUSION

In this study, TDC-based bidirectional DC-DC converter is designed and implemented for a lithium-ion battery. Control-

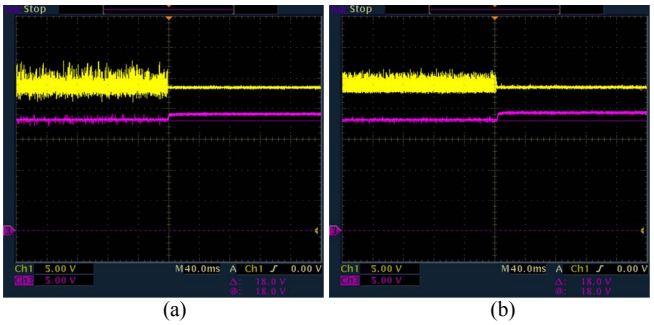

(a) (b)

Fig. 11. Bidirectional converter reference voltage change performance on buck mode operation by experiment: (a) PI control; (b) TDC.

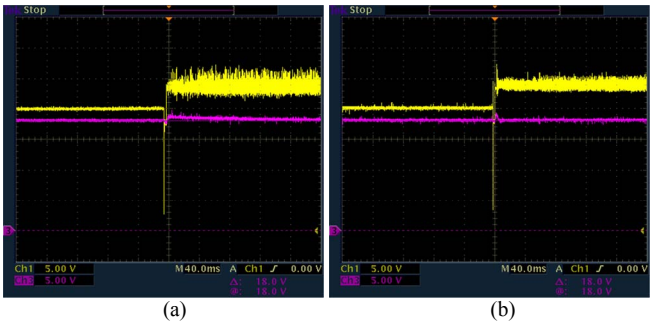

(a) (b)

Fig. 12. Bidirectional converter DC link bus voltage change performance on buck mode operation by experiment: (a) PI control; (b) TDC.

oriented model of the system is firstly constructed in MATLAB/Simulink. To regulate bus voltage and/or battery charge voltage, TDC is selected to remedy highly non-linear dynamical system characteristics. To validate TDC efficacy, PI control is also developed and compared. Numerical simulation and experimental implementation are tested based on five different operating conditions. TDC shows much better tracking performance with shorter settling time, and smaller ripples and overshoot in comparison with the PI control. Therefore, TDC is suitable for regulating bidirectional DC-DC converter for the application of a lithium-ion battery. TDC will be applied for more complex renewable energy system power conditioning in the future.

ACKNOWLEDGMENT

This work was supported by the National Research Foundation of Korea (NRF) funded by the Ministry of Education (2013-0005339), and by the Brain Korea 21 PLUS (BK 21+).

REFERENCES

[1] R.-J. Wai, R.-Y. Duan, and K.-H. Jheng, "High-efficiency bidirectional dc–dc converter with high-voltage gain," *IET Power Electron.*, vol. 5, no. 2, pp. 173–184, Apr. 2012.

[2] W. Na and B. Guo, "Analysis and control of bidirectional dc/dc converter for PEM fuel cell applications," in *Proc. 2008 IEEE Power and Energy Society General Meeting*, pp. 1–7.

[3] K. Jin, X. Ruan, M. Yang, and M. Xu, "Power management for fuel-cell power system cold tart," *IEEE Trans. Power Electron.*, vol. 24, no. 10, pp. 2391–2395, Oct. 2009.

[4] J. Park and S. Choi, "Design and control of a bidirectional resonant dc–dc converter for automotive engine/battery hybrid power generators," *IEEE Trans. Power Electron.*, vol. 29, no. 7, pp. 3748–3757, Jul. 2014.

[5] D. Kim, S. Choi, S. Kim, and B. Choi, "MATLAB-based digital design of current mode control for multi-module bidirectional battery charging/discharging converters," in *Proc. 2011 IEEE 8th Int. Conf. on Power Electronics and ECCE Asia*, pp. 2256–2260.

[6] S.-i. Hamasaki, R. Mukai, and M. Tsuji , "Control of power leveling unit with super capacitor using bidirectional buck/boost dc/dc converter," in *Proc. 2012 IEEE Int. Conf. on Renewable Energy Research and Applications*, pp. 1–6.

[7] S. Njoya Motapon, L.-A. Dessaint, and K. Al-Haddad, "A comparative study of energy management schemes for a fuel cell hybrid emergency power system of more electric aircraft," *IEEE Trans. Ind. Electron.*, vol. 61, no. 3, pp. 1320–1334, Mar. 2014.

[8] L. Wang, E. G. Collins, Jr., and H. Li, "Optimal design and real-time control for energy management in electric vehicles," *IEEE Trans. Veh. Technol.*, vol. 60, no. 4, pp. 1419–1429, May 2011.

[9] F. Ciccarelli and D. Lauria, "Sliding-mode control of bidirectional dc-dc converter for supercapacitor energy storage applications," in *Proc. 2012 IEEE Int. Symposium on Power Electronics Electrical Drives Automation and Motion*, pp. 1119–1122.

[10] D.-S. Oh, Y.-J. Kim, J.-D. La, and Y.-S. Kim, "The sliding mode controller of the bidirectional converter for the dc bus stabilization," in *Proc. 2012 IEEE Int. Conf. on Electrical Machines and Systems*, pp. 367–371.

[11] M. Ebad and B.-M. Song, "Accurate model predictive control of bidirectional dc-dc converters for dc distributed power systems," in *Proc. 2012 IEEE Power and Energy Society General Meeting*, pp. 1–8.

[12] Y.-P. Ko, Y.-S. Lee, and W.-H. Chao, "Analysis, design and implementation of fuzzy logic controlled quasi-resonant zero-current switching switched-capacitor bidirectional converter," *IET Power Electron.*, vol. 4, no. 6, pp. 683–692, Apr. 2012.

[13] A.S. Samosir and A. H. M. Yatim, "Dynamic evolution control of bidirectional dc-dc converter for interfacing ultracapacitor energy storage to fuel cell electric vehicle system," in *Proc. 2008 IEEE Power Engineering Conf.*, pp. 1–6.

[14] A.S. Samosir and A. H. M. Yatim, "Implementation of dynamic evolution control of bidirectional dc–dc converter for interfacing ultracapacitor energy storage to fuel-cell system," *IEEE Trans. Ind. Electron.*, vol. 57, no. 10, pp. 3468–3473, Oct. 2010.

[15] A.P.N. Tahim, D. J. Pagano, and E. Ponce, "Nonlinear control of dc-dc bidirectional converters in stand-alone dc microgrids," in *Proc. 2012 51st IEEE Conf. on Decision and Control*, pp. 3068–3073.

[16] K. Engelen, S.D. Breucker, P. Tant, and J. Driesen, "Gain scheduling control of a bidirectional dc–dc converter with large dead-time," *IET Power Electron.*, vol. 7, no. 3, pp. 480–488, 2014.

[17] K. Youcef-Toumi and O. Ito, "A time delay controller for systems with unknown dynamics," *ASME J. Dyn. Syst., Meas., Control*, vol. 112, pp. 133–142, Mar. 1990.

[18] Y.-X. Wang, D.-H. Yu, and Y.-B. Kim, "Robust time-delay control for the dc–dc boost converter," *IEEE Trans. Ind. Electron.*, vol. 61, no. 9, pp. 4829–4837, Sep. 2014.

[19] Y.-X. Wang, D.-H. Yu, S.-A. Chen, and Y.-B. Kim, "Robust dc/dc converter control for polymer electrolyte membrane fuel cell application," *J. Power Sources*, vol. 261, pp. 292–305, Sep. 2014.

[20] O. Tremblay, L.-A. Dessaint, and A.-I. Dekkiche, "A generic battery model for the dynamic simulation of hybrid electric vehicles", in *Proc. 2007 IEEE Vehicle Power and Propulsion Conf.*, pp. 284–289.